Tribological improvement of moving microparts by application of thin films and micropatterning

2008 J. Phys.: Condens. Matter 20 354018

(http://iopscience.iop.org/0953-8984/20/35/354018)

J. Phys.: Condens. Matter **20** (2008) 354018 (9pp) doi:10.1088/0953-8984/20/35/354018

Tribological improvement of moving microparts by application of thin films and micropatterning

R Bandorf, D M Paulkowski, K I Schiffmann and R L A Küster

Fraunhofer Institute for Surface Engineering and Thin Films IST, Bienroder Weg 54E, D-38108 Braunschweig, Germany

Received 31 January 2008, in final form 27 June 2008
Published 11 August 2008
Online at stacks.iop.org/JPhysCM/20/354018

Abstract

The relevance of active microsystems continually increases and with the expansion of applications also aspects of reliability and durability of the moving microparts. In particular, the microtribological improvement of active MEMS therefore was investigated and improved. On the one hand, the influence of different thin films was investigated; on the other hand, improvement by micropatterning of the tribological surfaces in combination with coatings was studied.

Most promising results were gained using thin carbon-based films. The typical film thickness of the coatings was in a range of several tens up to a few hundred nanometres. The films were deposited by plasma processes varying different process parameters, mainly the applied bias voltage. Different doping elements (Si, Au and W) were added to the diamond-like carbon (DLC) films (a-C, a-C:H, a-C:H:Si, a-C:H:Au, and a-C:H:W). Different methods were used for characterizing the thin films. Under single asperity contact indentation and scratch tests were performed to determine microhardness, microwear and microfriction. An influence of the applied bias voltage on the micromechanical and microtribological properties was found. At low constant loads of 100 μN the more brittle a-C films showed an initially higher microwear volume than the more elastic a-C:H films. With increasing load the microwear of the a-C films showed less increase of microwear compared to a-C:H films. At low load in the range from 50 μN to a few 100 μN the friction coefficient in single-asperity contact decreased with increasing load. Reaching a critical load the behaviour changed and due to inelastic effects, the friction coefficient increased with further increasing load.

For investigation of microabrasive wear under multi-asperity contact a specifically developed tester was used. Besides a ranking of different materials regarding their abrasive microwear resistance the influence of the substrate material on the resulting wear behaviour was investigated for tungsten-doped a-C:H films on silicon and polymer substrates. Using a softer substrate material the abrasive wear resistance for constant normal loading was doubled. Furthermore the friction coefficients of the films were determined by a pin-on-disc test and a specifically developed oscillating friction and wear tester working at flat-to-flat microcontact.

It turned out that the friction coefficient was strongly dependent on the resulting contact pressure. Therefore the contact area was modified by micropatterning. The resulting friction coefficient of the patterned samples was significantly lower compared to results for full area contact, depending on the structures used and resulting local pressure. Different geometric patterns were investigated. A reduction of the friction coefficient from 0.09 to 0.04 was measured for a-C-coated silicon on increasing the local pressure from 12.5 to nearly 600 kPa by micropatterning.

1. Introduction

Thin microtribological coatings are today investigated and to some extent already used to improve microtribological properties of micro-electromechanical systems (MEMS) [1–8]. Since adhesion has a huge influence on the microtribological behaviour most investigations focus on dry lubrication [9]. Typical thicknesses are in the range of a few nanometres for applications in hard discs [10, 11] as well as a few microns for macroscopic applications [12]. Due to the small forces, but high local pressures in MEMS components important R&D work is focused on wear-resistant surfaces with minimized friction and low stick–slip behaviour [13–16]. Due to the modified geometry and contact situation of microsystems several aspects of microtribology must be considered [10, 17–19]. Besides the selection of the coating material also specific adaptation of the preparation conditions as well as further optimization by micropatterning of the sample surfaces can lead to enhanced tribological properties [20, 21]. The microwear behaviour of a coated substrate is strongly dependent on both the mechanical properties of the substrate material and the coating.

2. Experimental details

2.1. Sample preparation

As substrates, flat samples of polished silicon as well as samples with different microstructures were investigated. The microstructures were generated by photolithography using AZ 6615 and AZ 4562 resin and reactive ion etching in an Ar/SF_6 plasma. The pattern size and structure were varied to realize different contact situations. For the pin-on-disc test concentric circles with varied spacing between the lines at a constant linewidth of 100 μm were prepared to vary the contact area, i.e. the resulting contact pressure (figure 1(a)). For the oscillating friction and wear tester two different microstructure geometries were investigated. On the one hand parallel lines with varied spacing at a constant linewidth of 10 μm were used (figure 1(b)). On the other hand microdots with varied spacing between the dots at a constant diameter of 12 μm were prepared (figure 1(c)). Figure 1 shows a schematic representation of the different microstructure geometries.

The Si substrates have been coated by different types of films (see table 1). All films were prepared in industrial sputtering plants. The base pressure was well below 1.0×10^{-5} mbar while the working pressure was 0.5×10^{-3} mbar. For the preparation of the alumina films rf sputtering, for cBN and a-C DC sputtering, for a-C:H, a-C:H:Si, and CN_x PACVD, and for a-C:H:W and a-C:H:Au combined PVD + PACVD was used. Table 1 gives an overview of the plasma gases and target materials used. The NiFe films were prepared by electroplating. The preparation parameters of the films are described in detail elsewhere [6, 29–32].

2.2. Analytical set-up

The micromechanical properties of the prepared films were determined using a Hysitron TriboScope™ [22–24] in conjunction with a Veeco Di3100 AFM. The TriboScope consists of a diamond tip that can be moved in two axes. A well-defined normal load can be applied to the tip and additionally the tip can be moved laterally. The resulting vertical and lateral displacement as well as the resulting friction forces can be measured as a function of time during the whole experiment. The typical loads for testing at single-asperity contact are 10 μN to 15 mN. For the determination of hardness of the films by indentation a Berkovich indenter with a tip radius of about 300 nm was used. For microwear and microfriction experiments conical diamond tips with 90° opening angle and tip radii between 0.6 and 6.5 μm were used. The experiments consist of either a single scratch with increasing load or an oscillating wear test under constant load condition for a predefined number of cycles.

Table 1. Film preparation for the following coatings: a-C = amorphous, hydrogen-free carbon, a-C:H = amorphous hydrocarbon, Al_2O_3 = alumina, CN*x* = carbonitride films, cBN = cubic boron nitride, a-C:H–W = tungsten containing hydrocarbon nanocomposite (contains WC nanoparticles), a-C:H–Au = gold containing hydrocarbon nanocomposite (contains Au nanoparticles), a-C:H–Si = silicon containing hydrocarbon coating.

Coating	Process	Process type	Plasma gas	Target
a-C	PVD	DC sputtering	Ar	Graphite
a-C:H	PACVD	Reactive sputtering	Ar, C_2H_2	—
Al_2O_3	PVD	RF-sputtering	Ar, O_2	Al_2O_3
CN_x	PACVD	Reactive sputtering	Ar, N_2	Graphite
cBN	PVD	DC sputtering	Ar, N_2	B_4C
a-C:H:W	PVD + PACVD	Combined DC + reactive	Ar, C_2H_2	W
a-C:H:Au	PVD + PACVD	Combined DC + reactive	Ar, C_2H_2	Au
a-C:H:Si	PACVD	Reactive sputtering	$C_4H_{12}Si$	—

In line with macroscopic investigations the other measuring instruments were testing under multi-asperity contact. The abrasive wear behaviour of the thin films was determined by a specifically developed abrasive wear tester, described in detail elsewhere [25, 26]. To realize a two-body contact a videotape as abrasive medium was moved under a loaded Al_2O_3 sphere grinding a crater in the sample surface. A load of 20 mN, a sliding speed of the videotape of 22 mm s^{-1}, and a counter body with 10 mm diameter was used. The resulting crater depths were determined by profilometry after grinding. The band length needed to grind a 100 nm deep crater was then used as the measure for abrasive wear.

For determination of the friction coefficient under multi-asperity contact conventional pin-on-disc tests were performed at a load of 3 N and a sliding speed of 40 mm s^{-1}. As counterparts balls (stainless steel, sapphire, and DLC coated steel) with 4.76 mm diameter were used.

For oscillating microfriction investigation samples were tested in flat-to-flat microcontact using a specifically developed oscillation testing machine described in detail elsewhere [27, 28]. The samples (10×10 mm^2) were mounted on a carrier performing oscillations with a maximum lateral displacement of 80 μm. DLC-coated Si(100) served as flat counterpart to the micropatterned test samples. The normal

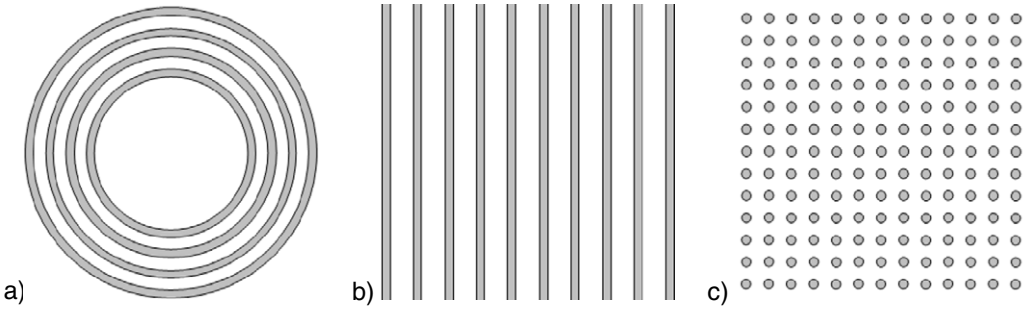

Figure 1. Schematic representation of the microstructure geometries of the patterned Si(100) substrate.

Table 2. Testing equipment: AFM system with Hysitron TriboScope, tape abrasive tester (TAT), pin-on-disc tester (POD) and oscillating friction tester (OFT).

Tester	Load (mN)	Tip radius (μm)	Shape	Speed (mm s^{-1})	Movement	Material
Hysitron Triboscope	0.01–15	0.3	3-sided pyramid (Berkovich)	—	Vertical indenting	Diamond
Hysitron Triboscope	0.01–2	0.6–6.5	Conical, 90°	0.001–0.01	Linear oscillating (scratch)	Diamond
TAT	20	5000	Sphere	22	Traverse winding tape	Videotape under Al_2O_3 sphere
POD	3000	2380	Sphere	40	Circular rotating	Stainless steel, sapphire, DLC coated steel
OFT	50–1000	—	Flat	0.16–5	Linear oscillating	a-C coated Si(100)

Table 3. Mechanical properties of the investigated microtribological films.

	Hardness (GPa)	Young's modulus (GPa)
a-C:H (dep. on bias)	24–30	170–270
a-C (dep. on bias)	15–50	150–500
CN_x (dep. on N content)	10–18	100–180
Al_2O_3	20–29	160–250
cBN	55–60	400–550

load was applied by deadweights in the range of 0.05–1 N. The resulting friction coefficient was measured by a quartz crystal sensor. Using oscillation frequencies up to 100 Hz, sliding speeds up to 5 mm s^{-1} were achieved. Table 2 gives an overview of the testing equipment used.

3. Results and discussion

3.1. Mechanical properties

Table 3 summarizes the hardness and Young's modulus of the investigated films. In particular for the carbon-based films (a-C, a-C:H, CN_x) the resulting mechanical properties strongly depend on the preparation parameters like bias voltage, gas mixture, and sp^3 fraction. The properties therefore can be tailored within a wide range as described in detail by Robertson [33].

The DLC films (a-C, a-C:H) exhibit a strong influence of the applied bias voltage on the resulting hardness. For hydrogen-free carbon films the hardness reached a maximum value of approximately 50 GPa at a bias voltage around −100 V. With further increase of the bias voltage the hardness decreased (figure 2(a)). With increasing bias voltage the growing film is more heavily bombarded by Ar ions, leading to a modification of the sp^2/sp^3 ratio and for high voltages, i.e. ion energies to graphitization of the films. For the hydrogenated films the maximum hardness of approximately 28 GPa was obtained at approximately −650 V bias voltage (figure 2(b)). It is well known that increasing the bias voltage increased the sp^3 fraction, leading to the rise in the hardness. Similar to a-C, graphitization of the a-C:H films occurs for very high voltages resulting in a reduced hardness. Furthermore for a-C:H the resulting properties strongly depend on additional parameters like the chamber size, position of gas inlet or gas composition (Ar/C_2H_2 ratio). For the a-C:H films a Balzers BAS 450 boxcoater was used at fixed inlet and constant gas mixture ratio. The film morphology of the a-C:H films changed with increasing bias voltage from a cauliflower-like structure (at low voltages) to a very smooth glassy structure (above −650 V), described in detail elsewhere [16]. Also the hydrogen content decreased with increasing bias voltage from 28% to 12%, measured by secondary ion mass spectroscopy (SIMS).

Besides the preparation parameters the substrate material and the film thickness also influence the resulting film properties of microtribological coatings (thickness < 1 μm). The thinner the films the more dominant becomes the substrate material. Figure 3 shows this influence of the substrate on the measured mechanical properties of thin films by

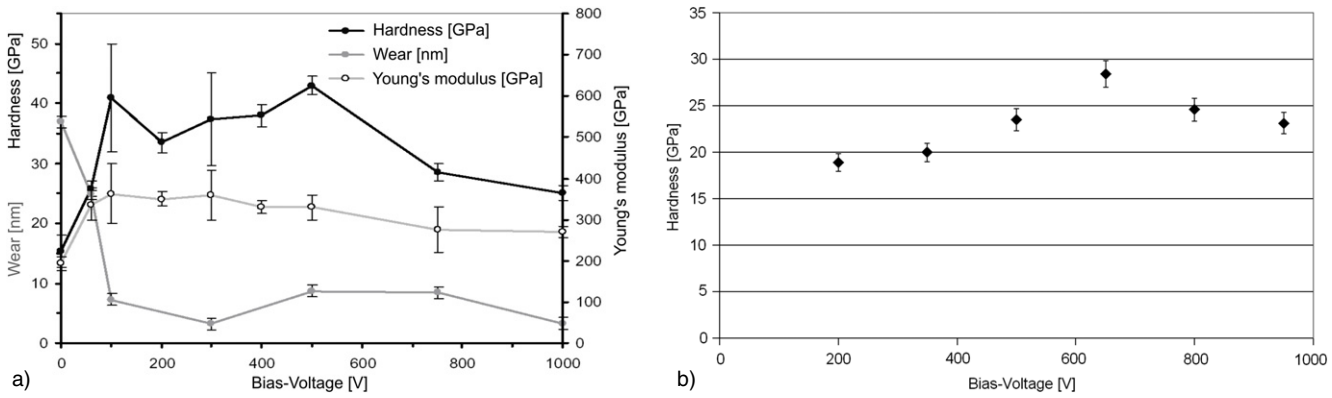

Figure 2. Influence of bias voltage on the resulting film hardness; (a) a-C, (b) a-C:H.

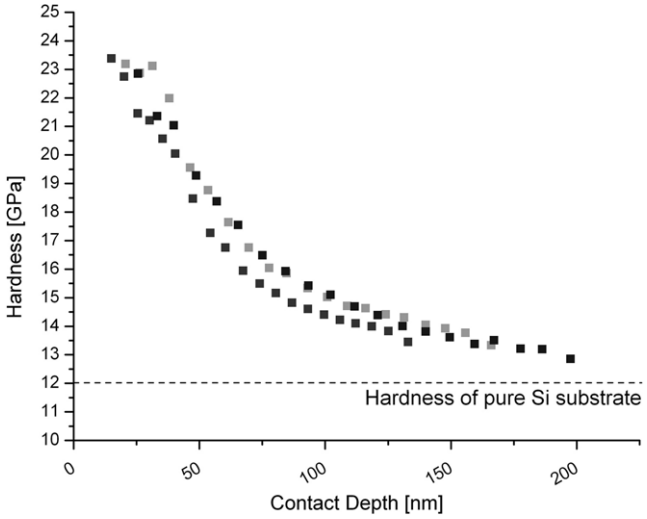

Figure 3. Hardness versus indentation depth of a 130 nm a-C coating with 10 nm Ti interlayer on Si(100), measured with a Berkovich indenter. With increasing indentation depth the hardness values approach the values of the silicon substrate.

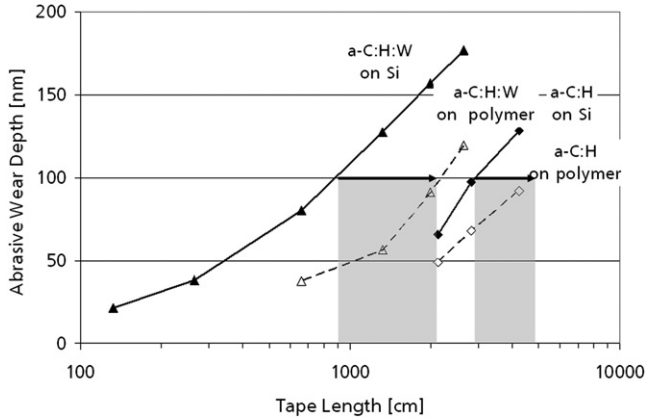

Figure 4. Influence of the substrate material on the resulting abrasive wear resistance. Horizontal indicators show the improvement of the tape length needed to grind a 100 nm deep crater in the surface.

nanoindentation. With increasing applied load of the indenter, i.e. increasing indentation depth, the influence of the substrate rises and the properties of the substrate material dominate the gained results. Only very low indentation depth of approximately 10 nm gained the real hardness value for the investigated film. For application it is important to adapt the film thickness to the resulting load to eliminate substrate effects.

For indentation measurements typically the 10% rule is used to avoid measuring the substrate influence [34]. Especially for thin films and soft substrate materials the influence can be even stronger. On the other hand, regarding the wear behaviour a soft substrate can improve the wear resistance due to modifying the effective loading and contact situation.

3.2. Wear behaviour of thin films

For determination of the abrasive wear of thin films the tape abrasive tester, described by Wortmann *et al*, was used [26]. A wide range from very soft (MoS_2) to very hard coatings (DLC, cBN, CN_x) were investigated and ranked regarding their abrasive wear resistance [29, 30]. It turned out that the carbon-based coatings obtained the highest abrasive wear resistance. Besides the ranking due to the wear resistance the influence of the substrate material was also investigated for a-C:H and a-C:H:W films on silicon as well as polymer substrates. Figure 4 shows that for constant applied load the abrasive wear resistance of DLC coatings could be increased by the use of soft substrate materials. Compared to silicon as substrate material the tape length needed to grind a 100 nm deep crater was twice as much, i.e. the abrasive wear resistance was twice as high for the same coating on the softer substrate. The higher wear resistance is due to elastic deformation of the polymer substrate, which increases the resulting contact area, resulting in a reduced contact pressure. This is possible since DLC coatings can support strong elastic deformations without crack formation or delamination from the substrate.

For the determination of microwear under single-asperity contact a Hysitron TriboScope under ambient conditions was used [22–24]. The remaining wear depth is a measure of the removed material as well as of densification or plastic deformation of the material [35, 36]. Figure 5 shows the resulting wear depth for different coating materials measured

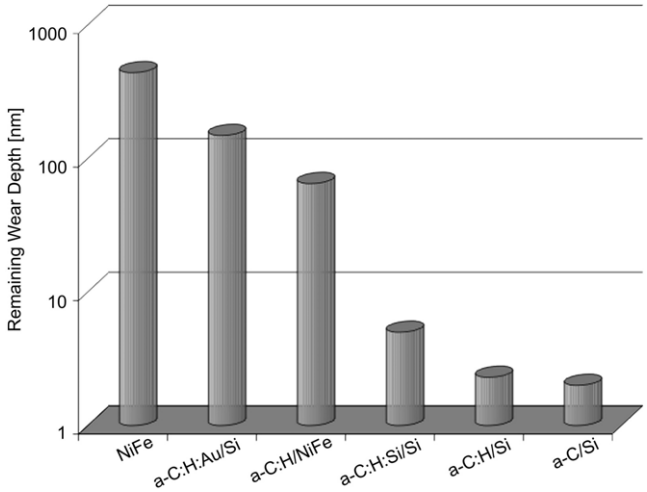

Figure 5. Remaining wear depth after oscillating microscratch test of different coating materials. Load 1 mN, 25 cycles, thickness of coatings 250 nm.

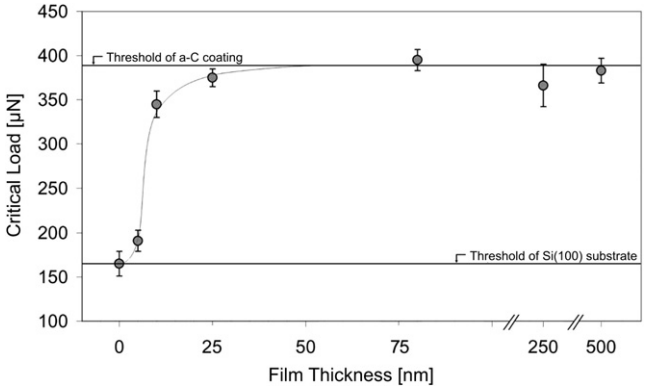

Figure 6. Influence of film thickness of a-C:H-coated Si substrate on the critical load, i.e. the onset of plastic deformation; single scratch with increasing load, conical diamond tip radius: 3 μm.

by an oscillating wear test under 1 mN load using a conical indenter with a tip radius of approximately 2 μm. In line with the results of the investigation of the mechanical properties the hardest films obtained the lowest abrasive wear.

Figure 6 shows the influence of the film thickness on the onset of plastic deformation. For determination of the critical load a single scratch test was performed, i.e. a diamond tip is laterally moved across the surface with linearly increasing load. Prior and after the scratch the surface topography is measured under minimum load. Therefore the onset of plastic deformation can be determined. While plastic deformation occurs at approximately 160 μN load for uncoated silicon only 5 nm a-C:H increases the limit to nearly 200 μN, resulting in a superposition of film and substrate effects. After applying a coating thickness of approximately 75 nm the critical load reaches a steady state. Therefore we conclude that for the 3 μm indenter with nearly 400 μN applied load we have reached the bulk properties of the a-C:H film.

In particular, thin films only a few tens of nanometres thickness exhibit an interesting behaviour. Figure 7 shows

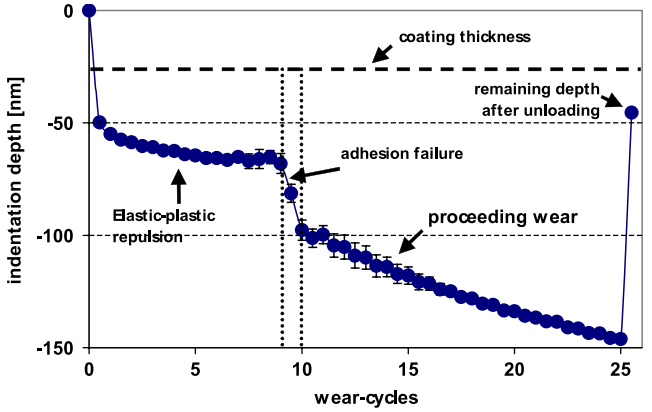

Figure 7. Oscillating wear test; 25 cycles, load: 0.5 mN, 25 nm a-C on Cu substrate. Vertical tip displacement during the test is shown. (This figure is in colour only in the electronic version)

an oscillating wear test of a 25 nm thick a-C coating on copper substrate at 0.5 mN applied load. Starting with the first cycle the resulting indentation depth is twice the film thickness. During the following cycles plastic deformation of the substrate increases while the film is still intact. After 10 cycles, the film breaks and the diamond scratches into the substrate. With the following oscillations the slope of the vertical displacement over cycle number changes and wear occurs. With every further cycle the indenter scratches deeper into the surface. After unloading the remaining wear depth is finally twice the coating thickness due to removal of material by scratching as well as plastic deformation of the softer Cu substrate during scratching [35]. Therefore a minimum film thickness depending on the film hardness is required for long term stability in MEMS applications.

Comparing the wear behaviour of a-C and a-C:H differences occurred correlated to the mechanical properties. For an applied load of 10 μN the more elastic a-C:H coatings showed no measurable wear at all, while a small remaining wear depth after oscillating scratching remained for the more brittle a-C films. With increasing load the behaviour changes and at 100 μN the remaining wear depth of a-C:H is more than twice the remaining wear depth of a-C after 10 cycles. While the initial wear during the first cycle is higher for a-C the further increase is small compared to a-C:H which obtained a smaller running-in behaviour but, especially at higher loads, the further generation of wear is higher [16]. Investigation of the elasto-plastic behaviour of the a-C and a-C:H films shows that there are three contributions to the z displacement. For its determination oscillating tests with an applied load of 2 mN and a diamond tip with 1 μm tip radius were used. The resulting wear can be separated into an elastic part that recovers after the test and plastic deformation during the tests, and true material loss. In absolute values the softer a-C:H coating obtains a slightly lower wear resistance with 65.6 nm remaining wear depth compared to 63.1 nm. Figure 8 shows the percentage of the three contributions for the two materials. It can be seen that the harder a-C coating obtains a higher fraction of material loss while the a-C:H film shows a larger contribution of elastic deformation recovering after loading.

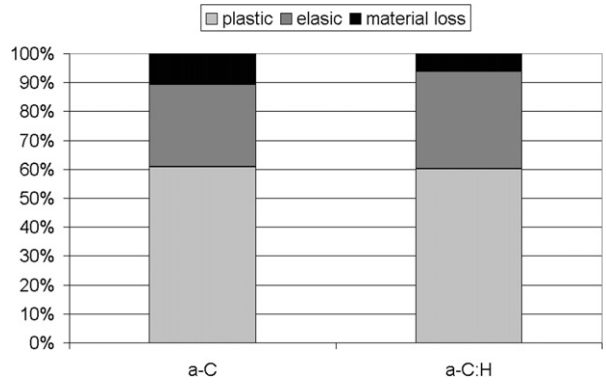

Figure 8. Elasto-plastic behaviour of 250 nm thick a-C and a-C:H films; portions of elastic and plastic deformation, and true material loss.

Table 4. Friction coefficient of different pairings, pin-on-disc, 3 N, ⌀: 4.76 mm, thickness approx. 1 μm.

	Counter body		
Coating	100Cr6	Sapphire	DLC-coated 100Cr6
Al_2O_3	0.89	0.54	0.15
cBN	0.46	0.45	0.12
CN_x	0.26	0.17	0.11
a-C:H	0.15	0.10	0.09
a-C:H:Au	—	0.28	0.09

3.3. Frictional behaviour of thin films

For determination of the friction coefficient under the macroscopic contact situation of the different tribological pairings the pin-on-disc test was used. As counterpart 100Cr6, sapphire and DLC-coated 100Cr6 balls with 4.76 mm diameter were used.

Table 4 summarizes the measured friction coefficients. The lowest values of all investigated coatings were measured in combination with DLC-coated 100Cr6 balls as counterpart. Very low friction coefficients $\mu < 0.1$ were measured only for DLC coatings in combination with DLC counterparts. For the DLC coatings a slight influence of the applied bias voltage was also visible, but the major effect was the choice of the mating materials.

Table 5 summarizes the microfriction coefficient and the remaining wear depth for different coatings at a constant load of 2 mN using a diamond indenter with 2.6 μm tip radius. Analogous to the pin-on-disc test the lowest friction coefficients and also nearly the lowest wear rates were measured for carbon-based systems. In particular for a-C an influence of the applied bias voltage on the microtribological properties was observed in addition. With increasing bias and therefore hardness (figure 2(a)) the friction coefficient increases and the wear resistance decreases. Optimized coatings regarding microtribological aspects and improved deposition rates were prepared at −100 V bias voltage.

Compared to the multi-asperity contact tests with pin-on-disc, the measured microfriction coefficients under single-asperity contact were typically lower. The major difference between micro- and macroeffects is due to the resulting contact

Table 5. Microfriction coefficient under single-asperity contact: load: 2 mN, conical indenter, tip radius 2.6 μm.

Coating		Microfriction coefficient, μ	Remaining wear depth (nm)
Al_2O_3		0.11	10.2
CN_x		0.12	15.0
cBN		0.10	—
a-C:H		0.07	1.2
a-C	Bias: 0 V	0.053	36.9
	− 60 V	0.057	24.9
	− 100 V	0.052	7.27
	− 300 V	0.069	2.7
	− 500 V	0.071	8.7

area. After Greenwood and Williamson the effective contact area for flat contacts increases with increasing load, thus compensating for each other will lead to a nearly constant friction coefficient [38]. For very smooth surfaces and single-asperity contact the behaviour differs. Applying Hertzian theory with increasing load the contact area increases much faster than the load. This leads to decreasing friction coefficients with increasing load. Therefore the friction coefficient under single-asperity contact is typically lower than macroscopically as long as no plastic deformation takes place [37].

Besides the frictional behaviour at multi-asperity contact the influence under single-asperity contact was also investigated using single and oscillating scratch tests with a conical diamond tip. Staedler *et al* [22, 23, 37] showed that there are at least three different stages existing that describe the microfrictional behaviour of very thin films in the range of a few tens of nanometres under single-asperity contact. Starting with low initial load the friction coefficient decreases during testing with increasing load due to increase in the Hertzian contact area. After reaching a critical load and minimum friction coefficient the friction coefficient starts to increase with further increasing applied load due to inelastic and plastic effects. Another change in the slope of the now rising friction coefficient with further increase of the applied load is finally observed when cracking of the coating occurs and the indenter finally starts to scratch into the substrate.

Basing on Staedler's results the influence of the counterpart radius, i.e. the resulting contact pressure for constant load was investigated starting at single-asperity contact using diamond tips with different radii, and ending with pin-on-disc tests realizing multi-asperity contact with ball diameters of a maximum 10 mm. The resulting friction coefficients of the investigations varying the contact area for spherical contacts is shown in figure 9. From the Hertz theory of elastic contact one would expect that the friction coefficient $\mu \sim R^{2/3}$, meaning that the smallest friction is found for the smallest contact radii, i.e. for the highest contact pressure, as long as no wear occurs. This is in fact, found even though the radius dependence is not $\sim R^{2/3}$. For the pin-on-disc test the friction coefficient is probably determined by plastic deformation and wear of microasperities.

Therefore, especially for MEMS surfaces, the frictional behaviour obviously can be tailored by modifying the contact

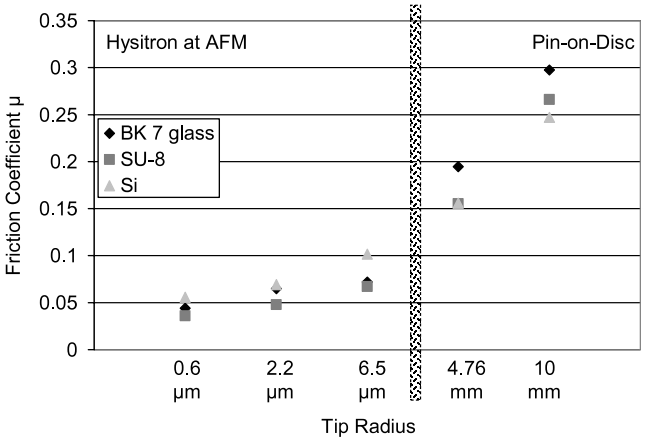

Figure 9. Friction coefficient of 250 nm a-C:H films on different substrate materials. Influence of tip radius of curvature. Hysitron tests performed at loads of 150 μN, pin-on-disc test at loads of 3 N.

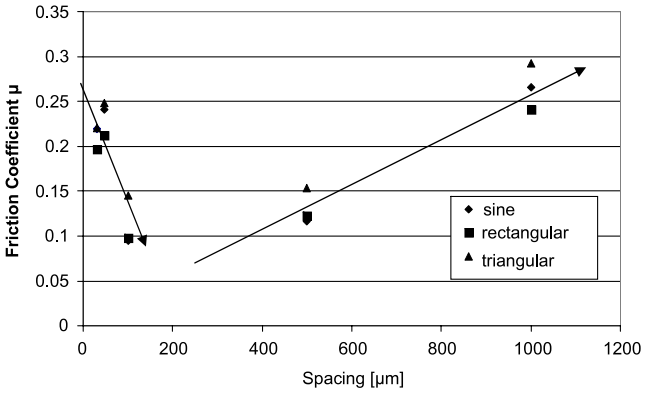

Figure 10. Friction coefficient of line structures in flat–flat microcontact; variation of spacing at constant linewidth of 10 μm; load: 0.2 N; a-C:H:Si on Si(100). The oscillating movement was applied by three different excitation signals: sine, rectangular and triangular.

area, resulting in changes of the local pressure. To improve this thesis different geometric patterned surfaces resulting in modified contact areas were investigated. Silicon substrates were micropatterned using photolithography and etching, followed by vacuum deposition of the investigated coatings on the patterned substrates. For areal contact a modification of the resulting percentage contact area was realized for pin-on-disc tests using substrates with a pattern of concentric circles to simulate behaviour of riding on rails. On modifying the contact area the friction coefficient compared to full area contact was reduced by 10% for a reduced contact area of approximately 75% [20]. A significantly higher reduction from $\mu = 0.25$ to 0.05 was measured for oscillating motion of small samples of approximately 10×10 mm^2. For line structures with 10 μm width the spacing was varied to modify the contact pressure. As figure 10 shows, with increasing spacing the friction coefficient decreases first. The increase in spacing between the lines correlates to the increase in contact pressure, as discussed for the single-asperity measurements. For spacing below 200 μm a reduction in the friction coefficient occurs.

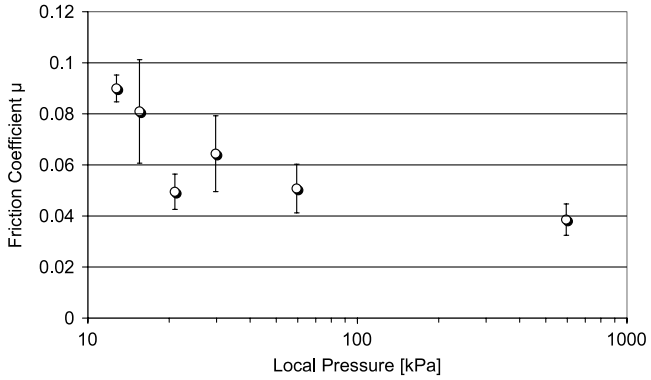

Figure 11. Influence of the local pressure on the resulting friction coefficient of microdots; 250 nm a-C on Si(100).

This correlates to the elastic deformation regime discussed by Staedler *et al* under single-asperity contact [37]. Between 500 and 1000 μm the friction coefficient rises again. Here inelastic and plastic effects occurred, i.e. increased wear was observed for the tested structures. It turned out furthermore that the lowest friction coefficients were measured for structured surfaces sliding against plain counterparts. For a resulting contact area of 5% of the nominal contact area, i.e. 10 μm lines with 200 μm spacing, extrapolation of the friction coefficient results in a reduction from $\mu = 0.25$ to $\mu < 0.1$ (figure 10). Using two patterned surfaces the structures get stuck to each other and consequently the friction coefficient rises [20].

Using microdots the friction coefficient was also reduced with increasing load, obviously not yet reaching the limit of plastic deformation of the support structure. For a structure of microdots with 12 μm diameter the spacing between the dots was varied, resulting in a variation of the contact pressure. Therefore with increasing spacing between the dots the friction coefficient was reduced from $\mu = 0.09$ to $\mu = 0.04$ for corresponding contact pressures of 12.75 kPa and 595 kPa, respectively (figure 11). Therefore tailored microtribological properties can be realized by optimizing coating thickness and surface structure.

It should also be mentioned for completeness that there is also a significant influence of humidity on the resulting microtribological behaviour, especially for carbon-based films [39, 40]. With increasing humidity the friction coefficient also increased for DLC films. The results on structured surfaces are already reported elsewhere [16]. It was seen that for microstructured surfaces the onset of the rise of the friction coefficient due to humidity is earlier compared to unpatterned samples.

3.4. Applications

The investigated coatings are used for microtribological improvement in moving microparts of microactuators fabricated within project SFB 516: construction and fabrication of active microsystems. One example is a rotatory microactuator. This microactuator consists of composite materials and magnetized polymeric magnet rotors. The tribological contact between rotor and stator was protected by the microtribological coating.

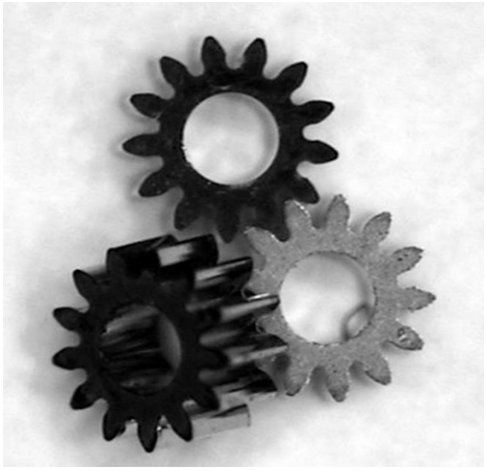

Figure 12. Microgears with DLC-coated flank side.

The low friction permits the operability of the actuator. The high wear resistance obtains a high reliability and increased lifetime. The integration of the composite materials, the magnetization of polymeric magnet rotors and the microtribological coating are of special interest for miniaturization down to diameters of 1 mm [41, 42].

Another application is coating LIGA microgears with a-C:H to increase the lifetime, i.e. improve the wear resistance of the system for use in microgearboxes (figure 12). Therefore a 250 nm thick a-C:H coating with hardness of 28.9 ± 3 GPa was applied. The lifetime of the gears was significantly increased as reported by Meyer *et al* [43].

4. Conclusion

Micromechanical as well as microtribological properties of different thin film materials were investigated under single- and multi-asperity contact situations. For microtribological use carbon-based coatings showed both very low microfriction coefficients and a high wear resistance. One major influence on the properties of the carbon-based films was the applied bias voltage during preparation. For optimized films, i.e. obtaining the greatest hardness the microtribological behaviour was studied in detail. While hydrogen-free carbon coatings (a-C) exhibit a larger initial wear the long term stability, especially at higher load exceeds the properties of a-C:H. For low loads, on the other hand the hydrogenated films can be applied running nearly wear-free.

Concerning the abrasive wear behaviour a ranking of several thin films was presented with the carbon-based films also showing the highest wear resistance. Furthermore the substrate material influences significantly the resulting abrasive wear behaviour. Therefore using softer substrate materials and thin films the wear resistance of the microtribological system can be improved due to a reduction of the effective contact pressure.

Concerning the microfriction of the investigated systems different aspects were discussed. Under single-asperity contact it turned out that the resulting friction coefficient is load-dependent, decreasing first with increasing load until inelastic and plastic effects occur, leading to a rise of the friction coefficient and finally to film failure. Thus, keeping in mind the load dependence a tailoring of the resulting contact area by micropatterning of the investigated substrates followed by application of the tribological coatings was investigated. Depending on the microstructures used and the resulting local pressure realized by the pattern size and distribution the friction coefficient under oscillation motion was decreased for an a-C:H:Si coated structure of parallel lines from $\mu = 0.25$ to less than 0.1 and for an a-C coated structure of microdots from $\mu = 0.09$ to 0.04, increasing the local pressure from 12.5 to nearly 600 kPa.

For improvement of MEMS and MEMS components the application of thin tribological films as protective coatings is favourable. For an optimized behaviour the influence of the substrate material used also has to be taken into account. Further improvement of the tribocontact can be yielded by adapting the resulting contact pressure using microstructured surfaces. Summarizing all these aspects well-tailored microtribological coatings are available for MEMS applications.

Acknowledgments

The authors acknowledge the financial support of the German Research Foundation by grant ‘SFB 516 Konstruktion und Fertigung aktiver Mikrosysteme’. We also thank all the Diploma and PhD students for their support for this paper.

References

[1] Wang W, Wang Y, Bao H, Xiong B and Bao M 2002 Friction and wear properties in MEMS *Sensors Actuators* A **97/98** 486–91
[2] Forbes I S and Wilson J I B 2002 Diamond and hard carbon films for microelectromechanical systems (MEMS)—a nanotribological study *Thin Solid Films* **420/421** 508–14
[3] Werner M R and Fahrner W R 2001 Review on materials, microsensors, systems and devices for high-temperature and harsh-environment applications *IEEE Trans. Ind. Electron.* **48** 249–57
[4] Erdemir A and Donnet C 2001 *Modern Tribology Handbook* vol II, ed B Bhushan (Boca Raton, FL: CRC Press) p 871
[5] Robertson J 2002 Diamond-like amorphous carbon *Mater. Sci. Eng.* R **R37** 129
[6] Bandorf R and Lüthje H 2002 Tribologische sub-mikrometer schichten für mikrosysteme *Vak. Forsch. Praxis* **14** 87–91
[7] Mani S S, Fleming J G and Sniegowski J J 1999 W-coatings for MEMS *Proc. SPIE Int. Soc. Opt. Eng.* **3874** 150–7
[8] Maboudian R and Carraro C 2004 Surface chemistry and tribology of MEMS *Annu. Rev. Phys. Chem.* **55** 35–54
[9] Sundararajan S 2001 Micro/nanoscale tribology and mechanics of components and coatings for MEMS *Thesis* Ohio State University
[10] Bhushan B 1999 Chemical, mechanical and tribological characterization of ultra-thin and hard amorphous carbon coatings as thin as 3.5 nm: recent developments *Diamond Relat. Mater.* **8** 1985
[11] Kulkarni A V and Bhushan B 1997 Nanoindentation measurements of amorphous carbon coatings *J. Mater. Res.* **10** 2707

[12] Lettington A H 1991 *Applications of Diamond Films and Related Materials* ed Y Tzeng *et al* (New York: Elsevier) p 703
[13] Bandorf R, Lüthje H, Schiffmann K, Beck M, Gatzen H H, Schmidt M, Büttgenbach S and Bräuer G 2004 Submicron coatings for micro-tribological applications *Microsyst. Technol.* **10** 223
[14] Bandorf R 2002 Ultradünne tribologische Schichtsysteme für elektromagnetische Mikroaktuatoren *Thesis* IST Berichte Nr. 15, (Stuttgart: IRB Verlag)
[15] Yasuhisa A and Jiro I 1996 Friction and pull-off force on silicon surface modified by FIB *Sensors Actuators* A **57** 83
[16] Bandorf R, Lüthje H, Henke C, Wiebe J, Sick J-H and Küster R 2005 Different carbon based thin films and their microtribological behaviour in MEMS applications *Surf. Coat. Technol.* **200** 1777
[17] Bandorf R, Lüthje H, Wortmann A, Staedler T and Wittorf R 2003 Influence of substrate material and topography on the tribological behaviour of submicron coatings *Surf. Coat. Technol.* **174/175** 461
[18] Liu E, Blanpain B, Shi X, Celis J-P, Tan H-S, Tay B-K, Cheah L-K and Roos J R 1998 Tribological behaviour of different diamond-like carbon materials *Surf. Coat. Technol.* **106** 72
[19] Zhang S, Bui X L and Fu Y 2003 Magnetron sputtered hard a-C coatings of very high toughness *Surf. Coat. Technol.* **167** 137
[20] Bandorf R, Lüthje H, Henke C, Sick J-H and Küster R 2004 Tribological behaviour of thin a-C and a-C:H films with different topographic structure under rotating and oscillating motion for dry lubrication *Surf. Coat. Technol.* **188/189** 530
[21] Dumitru G, Romano V, Weber H-P, Senstis M, Hermann J, Bruneau S, Marine W, Haefke H and Gerbig Y 2003 Laser treatment of tribological DLC films *Diamond Relat. Mater.* **12** 1034
[22] Staedler T 2001 Mechanische und tribologische Charakterisierung dünner Schichten mit Hilfe rastersondenbasierter Verfahren *Thesis* IST Berichte Nr. 12, IRB Verlag Stuttgart Fraunhofer
[23] Staedler T and Schiffmann K 2001 Correlation of nanomechanical and nanotribological behaviour of thin DLC coatings on different substrates *Surf. Sci.* **482–485** 1125
[24] Pape F, Küster R, Bandorf R, Bräuer G and Gatzen H H 2007 Nano-scratch studies on diamond-like carbon coatings on various materials applied in micro actuators *GFT Tribologie-Fachrichtung 2007* 1 (Göttingen, Germany) 28/1-28/10
[25] Wortmann A 2002 Entwicklung einer Prüfmethode zur meßtechnischen evaluation abrasiver Verschleißresistenz auf der Mikroskala *Thesis* IST Berichte Nr. 17, IRB Verlag Stuttgart Fraunhofer
[26] Wortmann A and Lüthje H 2000 *Proc. Materials Week 2000 (Munich)*
[27] Schmidt M, Wortmann A, Lüthje H and Büttgenbach S 2001 Novel equipment for friction force measurement on MEMS and micro components *SPIE Int. Soc. Opt. Eng.* **4407** 158
[28] Phataralaoha A and Büttgenbach S 2004 Microscopic friction force measuring system for the investigation of micro components *Proc. 4th Euspen Conf.* p 310
[29] Bandorf R, Lüthje H, Schiffmann K, Beck M, Gatzen H H, Schmidt M, Büttgenbach S and Bräuer G 2003 Submikrometerschichten für mikrotribologische Anwendungen *SFB-Kolloquium* (Braunschweig: Vulkan) pp 75–83
[30] Bandorf R, Lüthje H, Schiffmann K, Staedler T and Wortmann A 2001 Sub-micron coatings with low friction and wear for micro actuators *Proc. Micro System Technologies (Düsseldorf)* pp 243–8
[31] Bandorf R, Lüthje H, Schiffmann K, Staedler T and Wortmann A 2002 Sub-micron coatings with low friction and wear for micro actuators *Microsyst. Technol.* **8** 51–4
[32] Bandorf R, Lüthje H, Schiffmann K, Beck M, Gatzen H H, Schmidt M, Büttgenbach S and Bräuer G 2004 Submicron coatings for micro-tribological applications *Microsyst. Technol.* **10** 223–26
[33] Robertson J 2002 Diamond-like amorphous carbon *Mater. Sci. Eng.* R **37** 129–281
[34] Standard Test for Microhardness of Materials, ASTM Standard Test Method E 384 *Annual Book of Standards 3.01* 1989 (West Conshohocken, PA: American Society for Testing and Materials) p 469
[35] Kuester R 2006 Mikrotribologische Untersuchungen dünner Schichten unter Anwendung rastersondenbasierter Verfahren *Thesis* IST Berichte Nr. 24, (Stuttgart: IRB Verlag)
[36] Kuester R L A and Schiffmann K I 2004 Nano-scratch testing on thin diamond-like carbon coatings for microactuators: friction, wear and elastic-plastic deformation *Int. J. Mater. Res. Z. Met.kd.* **95** 306–10
[37] Staedler T and Schiffmann K 2001 Micromechanical and microtribological properties of thin CNx and DLC coatings *Adv. Eng. Mater.* **5** 333–7
[38] Greenwood J A and Wiliamson J B P 1966 Contact of nominally flat surfaces *Proc. R. Soc. Lond.* **295** 300
[39] Bhushan B 1999 Nanoscale tribophysics and tribomechanics *Wear* **225–229** 465–92
[40] Bhushan B 1999 Chemical, mechanical and tribological characterization of ultra-thin and hard amorphous carbon coatings as thin as 3.5 nm: recent developments *Diamond Relat. Mater.* **8** 1985–2015
[41] Waldschnik A, Feldmann M and Büttgenbach S 2007 Entwicklung von Synchron-Mikromotoren mit speziellen Rotoren basierend auf Polymermagneten *Mikrosystemtechnik Kongress 2007 (Dresden, Deutschland)* pp 295–8
[42] Ruffert C, Feldmann M, Waldschik A, Büttgenbach S and Gatzen H-H 2007 Fertigung von Antriebs-und Führungskomponenten für Mikromotoren *Kolloquium Mikroproduktion: Fortschritte, Verfahren, Anwendungen 2007 (Karlsruhe)* pp 165–70
[43] Meyer P, Klein O, Arendt M, Saile V and Schulz J 2006 Launching into a golden age (3)-gears for micromotors made by LIG(A) process *COMS 2006: Proc. 11th Annual Int. Conf. of Micro and Nano Systems (St. Petersburg, FL)*